Modeling of leakage mechanisms in sub-50 nm p^+-n junctions

Erin C. Jones and Nathan W. Cheung
Department of Electrical Engineering and Computer Sciences, University of California, Berkeley, California 94720-1772

(Received 21 February 1995; accepted 2 August 1995)

High leakage currents of ultrashallow junctions formed by B diffusion out of solid-phase epitaxially grown $CoSi_2$ contacts grown from Co/Ti bilayers on Si are explained by the Shannon contact model. Depending on implant condition, the diodes behave either as p-n diodes or Schottky diodes with barrier height enhanced by the p-type diffusion. Diodes implanted with $^{11}B^+$ at 7.5 keV and 10^{15} cm^{-2} dose show leakage current near 100 nA/cm^2 at -5 V and behave like ideal p-n junctions after a 900 °C, 30 s postimplant anneal. Diodes implanted at 3.5 keV with 10^{15} cm^{-2} dose or at 7.5 keV with a 10^{14} cm^{-2} dose display higher leakage currents and other characteristics like Schottky diodes. Further analysis of the Shannon contact model shows that thermionic emission leakage current of Schottky-like diodes may limit p-n junction scaling: with p-type doping concentrations of 10^{18}–10^{19} cm^{-3}, the Shannon contact model predicts that a 20–30 nm p-type junction depth below metal contacts is necessary to keep leakage at acceptable levels. A capacitance–voltage method is suggested for finding the minimum junction depth of p-n junctions. © *1996 American Vacuum Society.*

I. INTRODUCTION

In upcoming generations of metal–oxide–semiconductor field-effect transistor (MOSFET) devices, it is expected that improvements in performance and speed will be made by the scaling down of device dimensions. Controlled reduction of critical device dimensions has become a major thrust in device manufacturing. For some device parameters, like gate oxide thickness, it has been acknowledged that fundamental scaling limits are being approached: a linear reduction of the thickness parameter cannot be done and still maintain material and device reliability. For the diffused source/drain junctions, no such limits have been acknowledged, as making junctions below 50 nm in junction depth that even approach fundamental limits has been difficult.

The reduction of shallow source/drain junction diffusion length is a critical problem in sub-micron MOSFET devices, where short-channel effects like drain-induced barrier lowering cause the threshold voltage to be a function of both applied voltage and lithographically defined channel length. Reproducible reduction of these effects is achieved by keeping the effective channel length as long as possible. Although reduction of the lateral source/drain diffusion junction depth is essential for threshold voltage control and reproducibility, its scaling has historically been less aggressive than the scaling of minimum feature size. This has been due to the difficulty in controlling the thermal budget in furnace annealing steps where significant diffusion occurs during heating and cooling of the large thermal mass of the furnace.

Since the advent of rapid thermal annealing (RTA) systems, shallow junction scaling to around 100 nm has become feasible. Sub-100 nm p^+ junctions have even been made with boron,[1,2] whose large diffusivity in Si is greatly enhanced in the presence of residual damage caused by the dopant implantation steps used to introduce the dopant. Reducing the junction depth to 60 nm and below is still difficult, but has been shown possible with standard processes by reducing the RTA thermal cycle. Junctions of 10–50 nm have been shown using P and As diffusion[3,4] and junctions of 60 nm have been shown with boron dopant.[2,5] Reducing the boron junction depths below 60 nm by standard processes requires further reduction of the thermal budget, and an even more difficult tradeoff between lateral and vertical junction depth, sheet resistance, contact resistivity, and reverse junction leakage currents. Dopant incorporation by implantation and thermal activation, diffusion from a gaseous source, and diffusion from a doped thin film are all subject to this compromise. One process investigated to circumvent the difficulty is the use of $CoSi_2$ as a dopant source. The $CoSi_2$ dopant source technique has two advantages: the dopant is implanted into the silicide, so there is no residual implant damage in the silicon, and lower thermal cycles can be used for diffusion. In addition, during p^+ diffusion, boron in the $CoSi_2$ segregates at the $CoSi_2$/Si interface, promoting the incorporation of B in the Si near the interface.

II. EXPERIMENT

The devices described here are epitaxial $CoSi_2$/p-Si/n-Si diode structures. Epitaxial $CoSi_2$ contacts (50 nm thick) are

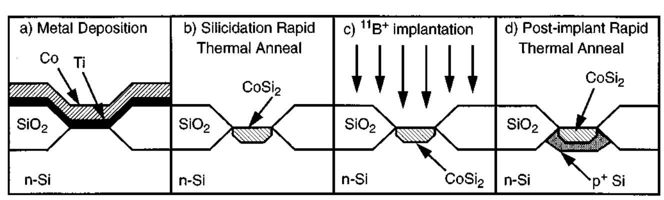

FIG. 1. Schematic drawing of $CoSi_2$ diode process flow: (a) deposition of 15 nm Co, 2 nm Ti bilayer, (b) solid-phase epitaxial growth of $CoSi_2$ in 900 °C, 30 s RTA, (c) implantation of boron into silicide, and (d) second RTA step at 900 °C, 30 s, to diffuse boron out of silicide.

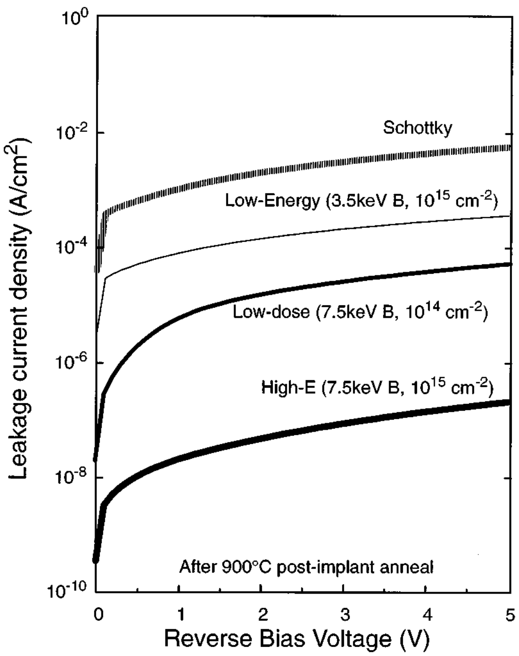

FIG. 2. Reverse-biased current density–voltage (JV) curve for diodes implanted with boron after 900 °C postimplant anneal, showing Schottky-like behavior of diodes implanted at a low-dose or low-energy condition and orders-of-magnitude variation in leakage current among samples. The high-energy, high-dose sample has the lowest leakage, about 100 nA/cm^2.

formed in local oxidation (LOCOS) oxide patterns on 8–12 Ω cm n-type Si as shown in Fig. 1. A sputter-deposited bilayer of 15 nm Co and 2 nm Ti is followed by a rapid thermal solid-phase epitaxy step. The silicide is then used as a dopant source for boron. Boron is implanted into the silicide at 3.5–7.5 keV implant energy and 10^{14}–10^{15} cm^{-2} dose. The naming conventions of the specific samples to be discussed are summarized in Table I. The details of the processing sequence were described previously.[6] Reverse-biased current density-voltage (JV) characteristics are shown for the diode samples after 900 °C annealing in N_2 RTA in Fig. 2. Orders-of-magnitude variation is observed in the reverse leakage currents despite secondary ion mass spectroscopy (SIMS) and spreading resistance profile data indicating that significant quantities of B are present under the silicide for all the samples. For comparison, Schottky diodes were made in the same silicide processing sequence but without the B implantation and annealing steps. In Fig. 2, the low-energy and low-dose JV curves show similar curve shapes but large differences in leakage magnitude from the Schottky diode curve. These shallow p-n junction characteristics lead to the description of the $CoSi_2$ diodes as Shannon contacts,[7] where the small amount of p-type dopant present effectively increases the Schottky barrier height and decreases the barrier height-dependent thermionic emission current observed. Diodes made by dopant out-diffusion at 900 °C have p layers[8] about 4–80 nm thick with peak doping of 10^{18}–10^{20} cm^{-3}. The models presented in this article will investigate the properties of junctions like these as a function of substrate and surface layer doping.

III. MODELING OF ULTRASHALLOW p^+-n JUNCTIONS

A. Shannon contact modeling of *IV* characteristics

When n-type dopants are used for shallow junction fabrication, sufficient dopant activation can be achieved in a short, low-temperature thermal cycle due to the high solid solubility and moderate diffusivity of n-type dopants like As and P in Si. Shallow n^+ junctions often exhibit tunneling leakage in the reverse bias region,[4,9] as the shallow junction depth is coupled with a high concentration of activated dopant. A shallow, highly doped junction causes large electric fields in the junction depletion region under reverse bias. This leads to significant tunneling current when the substrate doping is high, as in MOSFET channel regions.

For p-type doping, the only dopant with high solubility is rapidly diffusing B, for which a shallow junction depth is usually tied to low activation in standard process sequences. In this case, the junctions may not behave as ideal p-n junctions, but rather as Shannon contacts.[7] A schematic drawing of the band diagrams and sources of current for the four likely current mechanisms is shown in Fig. 3. The Shannon contact is a Schottky metal–semiconductor contact with a barrier height enhanced by a thin layer of Si doped oppositely to the substrate under the metal. At the point where the p-n junction becomes shallow enough to be described as a Shannon contact, its leakage increases rapidly.

A schematic of the Shannon contact doping profile and band diagram is shown in Fig. 4. The thin p layer of thickness, d, is assumed here to have a constant doping profile with net dopant concentration N_A, for simplicity. If image force lowering of the barrier is ignored and the p layer is fully depleted, the thermionic emission barrier height is the sum of the barrier height of the metal contact to n-Si plus the enhancement due to the p layer:

$$\Phi_B(V) = \Phi_{B0} + \Delta\Phi(V), \tag{1}$$

where the enhancement $\Delta\Phi$ is a function of the p-layer doping, junction depth, substrate doping, temperature, and applied voltage. In this work, the Φ_{B0} used is the zero-bias $CoSi_2$ to n-Si barrier height of the epitaxial $CoSi_2$ material used, which was measured at 0.72 eV from the $CoSi_2$/n-Si Schottky diodes described in the preceding section.

In this model, when the p-layer doping and thickness become high enough, the total barrier height to n-Si will saturate. Saturation occurs when the band bending between the p-Si and n-Si reaches its maximum value, $E_g - \Phi_n - \Phi_p$ at thermal equilibrium, where Φ_n is $E_c - E_f$ in the quasineutral n-type substrate and Φ_p is $E_f - E_v$ in the quasineutral region of the diffused layer. When the barrier height saturates, holes

TABLE I. Energy and dose of boron implant.

Sample	High energy	Low energy	Low dose
Implant energy	7.5 keV	3.5 keV	7.5 keV
Implant dose	10^{15} cm^{-2}	10^{15} cm^{-2}	10^{14} cm^{-2}

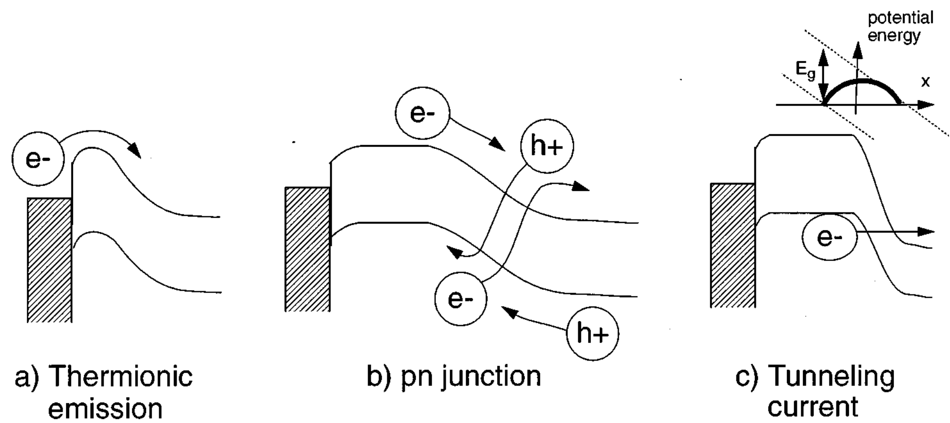

FIG. 3. Band diagrams and sources of reverse-biased leakage current in three types of junctions: (a) Schottky/Shannon contact leaks due to thermionic emission of electrons from metal into n-Si, (b) p-n junction diode leakage is due to both hole and electron generation in the junction depletion region and minority carrier diffusion across junction, and (c) tunneling leakage in reverse bias consists mostly of electrons from valence band tunneling into valence band on the n-type side. The parabolic barrier used is shown. Ohmic contacts are assumed at the silicide/Si interface for (b) and (c).

begin to build up in the area of the peak potential, and the layer can no longer be assumed fully depleted. This is one measure of when the device begins to behave like a p-n junction. The barrier height enhancement is calculated from Poisson's equation, assuming complete depletion of the surface layer. Assuming that the surface potential is Φ_{B0} and the potential in the bulk is $\Phi_{B0}-(V_{\mathrm{BI}}-V)$, the total depletion width W is found:

$$W(V)=\left[\frac{2\epsilon_S}{qN_D}(V_{\mathrm{BI}}-V)+d^2\left(1+\frac{N_A}{N_D}\right)\right]^{1/2}, \tag{2}$$

where V_{BI} is the built-in potential as described in Fig. 4. The increase in barrier height is then described by

$$\Delta\Phi(V)=\frac{q}{2\epsilon_S}\left(\frac{N_D^2}{N_A}(W-d)^2-2N_Dd(W-d)+N_Ad^2\right). \tag{3}$$

The current density–voltage characteristic of the Shannon contact is dominated by thermionic emission current, like a Schottky contact, but the enhanced barrier height is used in the current equation:

$$J_{\mathrm{SC}}=A^*T^2\exp\left(\frac{-q\Phi_B(V)}{kT}\right)\left[\exp\left(\frac{qV}{kT}\right)-1\right], \tag{4}$$

where A^* is the effective Richardson constant for n-type Si, 252 A/(cm^2 K^2). As shown in Ref. 7, for moderate doping levels, the magnitude of the current density is sensitive to very small changes in the junction depth. A small, 5 nm thickness variation causes a factor of 1000 increase in leakage at -3.3 V of a 30 nm junction with junction doping of 10^{18} cm^{-3} and background doping of 10^{16} cm^{-3}. At the point where the barrier height saturates, when the band bending has reached its maximum, the thermionic emission leakage drops to the pA/cm^2 level according to this model.

To determine how shallow a junction can be tolerated at different doping levels, the leakage current density is plotted as a function of the p-layer thickness for varying p-layer doping concentration, N_A, with substrate doping of 10^{16} cm^{-3} in Fig. 5(a) and 10^{18} cm^{-3} in Fig. 5(b). The figures show the threshold p-type material thickness to make a low-leakage p-n junction when the substrate doping increases,

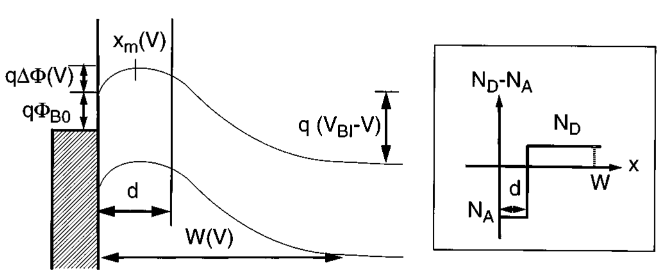

FIG. 4. Schematic drawing of the Shannon contact band diagram. $q\Phi_{B0}$ is the barrier height of the Schottky diode (with no p-type doping layer) at zero bias. $q\Delta\Phi(V)$ is the voltage-dependent enhancement in the effective barrier height due to the dopant profile shown in the inset. N_A and N_D are net dopant concentrations after compensation.

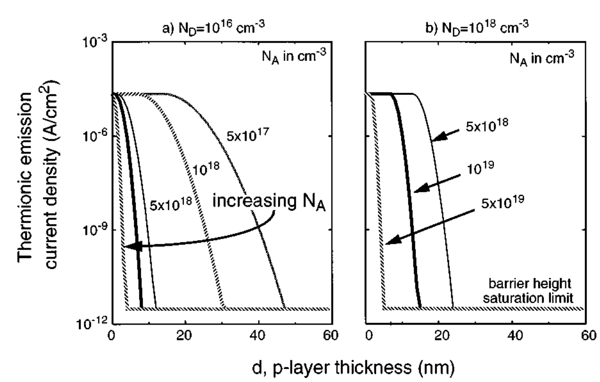

FIG. 5. Variation in the simulated thermionic emission current density at -3.3 V reverse bias with an increase in thickness and doping of the p layer under $CoSi_2$ contact for substrate doping of (a) 10^{16} cm^{-3} and (b) 10^{18} cm^{-3}.

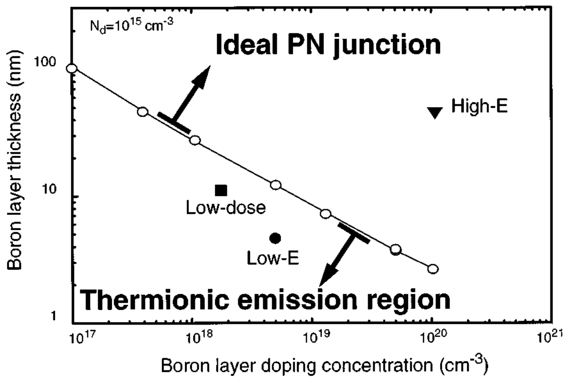

FIG. 6. Position of fabricated $CoSi_2$ device parameters in Shannon/p-n junction phase space. The boundary line gives the thickness and doping of the p layer to drop the thermionic emission current to 1 nA/cm^2. The substrate doping $N_D = 10^{15}$ cm^{-3}.

and the large sensitivity of the current to changes in doping. As N_A decreases from 5×10^{18} to 10^{18} cm^{-3}, the layer thickness required to drop the leakage below 1 nA/cm^2, a standard figure of merit for shallow junction leakage, doubles. According to this model, a shallow junction abutting a MOSFET channel region with doping near 10^{18} cm^{-3} requires more than 25 nm of material doped 5×10^{18} cm^{-3} or more to avoid thermionic emission leakage. If activation above 10^{19} cm^{-3} is possible, a 15 nm layer may be sufficient to meet the leakage requirement. If image force lowering is considered, the required junction depths are larger.

B. *p-n* junction/Shannon contact phase space

Ideal p-n junction leakage current includes the contributions of diffusion current and space-charge generation current. For most practical diodes, generation current is the limiting quantity, as the carrier generation and recombination lifetimes are determined by difficult-to-avoid, process-induced deep-level centers from heavy metal contamination, crystal damage, and mechanical stresses near the junction in a real diode. The total, ideal p-n junction current is given by

$$J_{p\text{-}n} = J_{\text{diff}} + J_{\text{gen}} = qn_i^2\left(\frac{1}{N_D}\sqrt{\frac{D_p}{\tau_p}} + \frac{1}{N_A}\frac{D_n}{d'}\right) + \frac{qn_iW}{\tau}, \tag{5}$$

where D_p and D_n are the diffusivity of holes and electrons, respectively, and d' is the quasineutral width of the p layer. The depletion width W used for the calculation is the Shannon contact depletion width when the barrier height enhancement is small and the normal p-n junction depletion width when the barrier height saturates. τ_n, τ_p, and τ are the leakage limiting lifetimes discussed above. As this current varies very slowly with changes in junction depth and doping, the p-n junction current in the following example is set to 1 nA/cm^2.

In Fig. 6, p-layer doping and thickness values obtained by spreading resistance profiling of the epitaxial $CoSi_2$ diodes are shown in the p-n junction/Shannon contact phase space. This graph shows the critical values of N_A and d of the

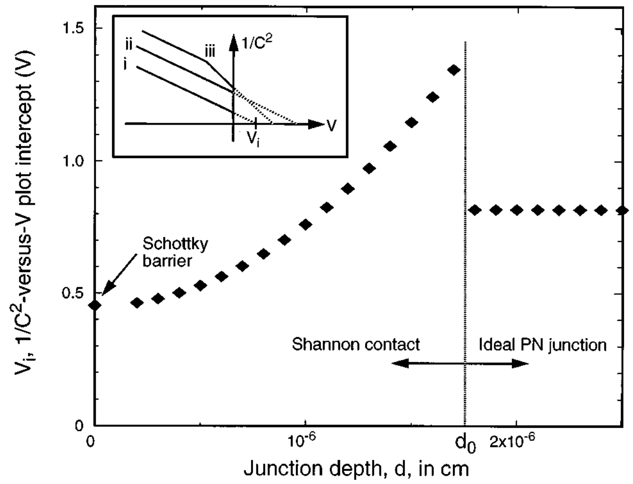

FIG. 7. Variation of the $1/C^2$ graph (shown in inset) intercept V_i with increasing junction depth d for constant diode doping $N_A = 2\times10^{18}$ cm^{-3} and background doping $N_D = 10^{15}$ cm^{-3}. The graph shows the gradual increase in the intercept as the dopant dose in Si increases and the fall in intercept when the p-n junction criterion is reached.

diffused layer necessary to keep the thermionic leakage current of a junction below 1 nA/cm^2. In a junction meeting this criterion, the leakage current is dominated by p-n junction generation current. The position in the diagram of the $CoSi_2$ diodes' thickness and doping data correlates very well with the leakage characteristics shown in Fig. 2. The low-energy and low-dose samples with high leakage and Schottky-like characteristics are located in the region where thermionic emission is the dominant leakage mechanism. The high-energy sample with leakage current density near 100 nA/cm^2 at -5 V is located above the cutoff line, in the region where diffusion and generation dominate, and can be described as a p-n junction.

C. *CV* characteristics

The Shannon contact behavior of the shallow diodes is also observed in capacitance–voltage measurements, where the presence of the depleted p-type layer makes the depletion region larger, and the capacitance smaller, than expected for a Schottky contact. Such capacitance–voltage measurements have been used to monitor the progression of dopant into semiconducting material, by observing the increase in the V-axis intercept of the $1/C^2$ versus V diagram after increasing thermal cycles.[10] In this work, we suggest that looking for the point where V_i, the V-axis intercept of the $1/C^2$ plot, drops back to the p-n junction value is one way to identify the p-n junction. The depletion width of the Shannon contact is given by Eq. (2). As $C = \epsilon_s A/W$, the intercept of the $1/C^2$ plot occurs where $1/C^2 = 0$, when

$$V_i = V_{\text{BI}} + \frac{q}{\epsilon_s}(N_A + N_D)d^2, \tag{6}$$

where $V_{\text{BI}} = \Phi_{B0} - \Phi_n$. The Schottky diode intercept is recovered by setting $d = 0$. V_i for the p-n junction is the

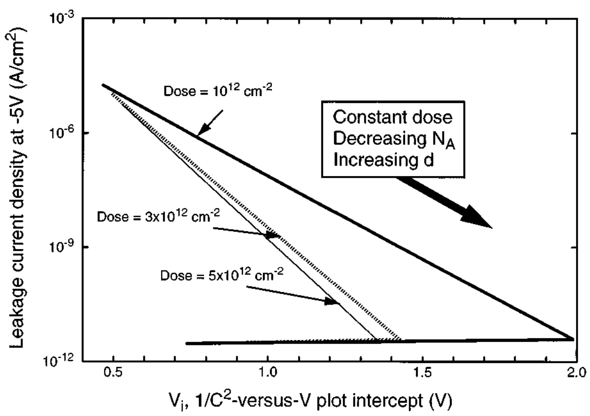

FIG. 8. The relation between leakage current density and the intercept of the $1/C^2$ diagram, V_i, shows leakage steadily decreasing as V_i increases and snapping back at the p-n junction condition. Successive points on the constant dose lines in the direction of the arrow have increasing junction depth and decreasing doping, showing that increasing the junction depth is most effective for reducing leakage and making a p-n junction.

built-in potential of the p-n junction, which varies slowly for N_A in the degenerate doping regime, and varies from around 0.75–0.85 V for $N_A = 10^{18}$–10^{20} cm^{-3} and $N_D = 10^{15}$ cm^{-3}, like the diodes studied. The variation in intercept V_i is shown in Fig. 7 for varying junction depth d. At $d=0$, the intercept is at the Schottky value. As d increases, the magnitude of the $1/C^2$ curve increases but the slope remains constant so the $1/C^2$ plot intercept increases, as shown in the inset of Fig. 7, line ii. The intercept increases until the barrier height saturates. When the saturation point is reached, the slope of the $1/C^2$ curve increases to the p-n junction value, and the intercept falls abruptly to the p-n junction built-in potential (Fig. 7 inset, line iii). For layers thicker than this, the p-n junction intercept will be constant. As shown in the inset of Fig. 7, however, if high enough voltage can be applied to deplete the p-type layer, the Shannon contact behavior may again be observed.

Plotting the thermionic emission reverse leakage current of Shannon contacts as described by Eq. (4) against the intercept V_i leads to Fig. 8, where the variation of leakage and intercept is shown as the dopant dose in Si increases. The line shows the initial increase in the intercept and reduction in leakage current as the barrier height enhancement increases. When the barrier height saturates and the diode begins to act as a p-n junction with a quasineutral region in the p-type layer, the intercept decreases to the built-in potential of the p-n junction. The three lines show the dependence of the diodes' behavior on the total dose of dopant in the junction. Along each line in the plot, the p layer has a constant dose. Successive points on the lines in the direction of the arrow have increased junction depth and decreasing doping N_A. The observation that increasing d and decreasing N_A is the way to reduce the leakage for junctions formed with a constant dose is another reason to limit shallow junction scaling. Increasing the junction depth is more efficient for reducing leakage. Observation of such an experimental curve may be useful for finding the minimum drive necessary to create a diode with p-n behavior, where leakage current is not so heavily dependent on and sensitive to changes in the junction depth and doping.

In Table II, the $1/C^2$ intercepts and leakage behavior of the $CoSi_2$ diodes are summarized. The results track well with Fig. 8. The low-energy diode shows a barrier height higher than the Schottky junction and reduced leakage. The low-dose diode shows an increased barrier height, but on average, no reduction in the leakage due to a very large spread in leakage among the low-dose samples, as expected from Fig. 5. The SIMS data of the best, lowest-leakage low-dose samples showed that those had a similar dose but higher junction depth of B in the Si than the low-energy samples.[8] This correlates with the trend seen in Fig. 7, where deeper junction depths are seen to be most effective for reducing leakage. For the high-energy diode, the intercept has decreased and the leakage has decreased further, showing it has reached the p-n junction regime.

D. Tunneling contact/Shannon contact phase space

New shallow junction fabrication technologies are first tested on diode test structures like the $CoSi_2$ diodes described in this article. For fabricating low-leakage diodes, high-purity wafers are used, which usually have substrate doping of 10^{15}–10^{16} cm^{-3}. The substrate doping found in MOSFET devices may range from these low values in the vertical direction under the junction to 10^{17}–10^{18} cm^{-3} in the lateral direction where the shallow junction meets the MOSFET channel region. N_A may range from the solid solubility at peak annealing temperatures, 3×10^{20} cm^{-3} at 1100 °C, down to levels only slightly greater than the substrate doping, if annealing is done at low temperatures to minimize the diffusion. As the doping can vary by a factor of 10^5 in a MOSFET device, different current mechanisms may dominate in different locations, depending on the doping levels.

TABLE II. Summary of CV and JV data of diodes.

Sample	High energy	Low dose	Low energy	Schottky
V_i, CV intercept (V)	0.76	1.07	0.82	0.45
Average leakage current density (μA/cm^2)	25	572	550	7000
Best leakage current density	100 nA/cm^2	22 μA/cm^2	350 μA/cm^2	2.3 mA/cm^2

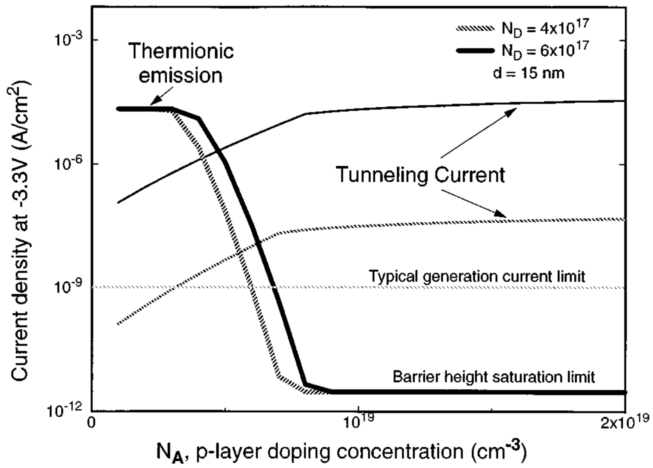

FIG. 9. Variation in simulated current densities of three diode types at -3.3 V, showing the importance of the thermionic emission current for p-layer doping of 5×10^{18} cm^{-3} and below. Tunneling current dominates when the p-layer doping is above that level and the substrate doping is high.

Tunneling currents have been detected in reverse-biased p-n junctions used in bipolar transistor emitter-base regions[9] and simulated MOSFET channel regions[4] where the doping concentrations and peak electric fields are high. These currents can be significant in MOSFET channel regions when the source and drain are reverse-biased. Expressions for reverse-biased diode tunneling current have been calculated using the WKB approximation to determine a tunneling transmission factor for the electrons.[11,12] In the reverse-biased region, only electrons tunneling from the valence band of the p layer into the n-type bulk are significant. Assuming a parabolic tunneling barrier (Fig. 3), the current density for a reverse-biased diode is described as

$$J_{\mathrm{TN}}=\frac{\pi q^2 m_r V E_g E_m}{h^3 E_0}\exp\left(-\frac{E_0}{E_m}\right), \tag{7}$$

where q is the electronic charge, h is Boltzmann's constant, E_g is the Si band gap, m_r is the effective mass value for the tunneling electron in an indirect band gap material,[12] and the quantity E_0 is a band gap and effective mass-dependent constant. When the p-type layer is fully depleted, the maximum electric field E_m is calculated using the depletion width given by Eq. (2), noting that the width of the positive space-charge layer on the n side is $W-d$. In the cases where the barrier height is saturated and the contact is more like an ideal p-n junction in nature, the depletion width is calculated as for a normal p-n junction and the space-charge layer width on the n side is $N_A W/(N_A+N_D)$.

The comparison of reverse leakage current mechanisms is shown in Fig. 9 as a function of N_A and N_D, with the junction depth fixed at 15 nm. Generation-limited p-n junction current density is again set equal to 1 nA/cm^2. As the tunneling current is very sensitive to doping levels, it is negligible until the substrate doping is above 10^{17} cm^{-3}. Even so, the thermionic emission leakage current is larger up to $N_A=10^{18}$ cm^{-3} for a $N_D=4\times10^{17}$ cm^{-3} and up to $N_A=4\times10^{18}$ cm^{-3} for $N_D=6\times10^{17}$ cm^{-3}. This simple model predicts that with substrate doping of $N_D=10^{18}$ cm^{-3}, a low-leakage ideal p-n junction characteristic cannot be achieved at all due to thermionic emission and tunneling leakage currents. Channel doping below 3×10^{17} cm^{-3} is sufficient to drop tunneling currents below the diffusion/generation levels in this simulation. To avoid tunneling leakage and to maintain low-leakage off-state characteristics of MOSFET devices, doping levels in the channel region are limited by this value.

IV. CONCLUSION

The preceding analysis indicates that there are strict limits on shallow junction depth and doping if junctions are to behave like ideal p-n diodes with low off-state leakage. The Shannon contact model has been used to provide a first-order estimate of the minimum junction depth of shallow source/drain diffusions that can be used for low-leakage MOSFET applications like dynamic memory. For shallower junctions, it is important that the metal contact be kept away from the junction, perhaps through the use of elevated source/drain structures. For ultrashallow p layers, the active doping concentration should be maximized and be kept above 10^{19} cm^{-3} to minimize thermionic emission leakage current, and substrate doping must be kept below 3×10^{17} cm^{-3} to avoid tunneling leakage.

ACKNOWLEDGMENTS

The authors wish to thank D. B. Fraser for helpful discussion and generous project support. This work has been supported by SEMATECH, Intel Corporation, the Intel Foundation, and the National Science Foundation (Grant No. ECS-9202993).

[1] E. C. Jones and N. W. Cheung, IEEE Electron Device Lett. **14**, 444 (1993).
[2] S. N. Hong, G. A. Ruggles, J. J. Wortman, E. R. Myers, and J. J. Hren, IEEE Trans. Electron Devices **38**, 28 (1991).
[3] M. Ono, M. Saito, T. Yoshitomi, C. Fiegna, T. Ohguro, and H. Iwai, in *Proceedings of the International Electron Device Meeting, 1993* (IEEE, Piscataway, NJ, 1993), Vol. 24, p. 119.
[4] B. G. Park, J. Bokor, H. S. Luftman, C. S. Rafferty, and M. R. Pinto, IEEE Electron Device Lett. **13**, 507 (1992).
[5] S. Ando, H. Horie, M. Imai, K. Oikawa, H. Kato, H. Ishiwari, and S. Hijiya, in *Proceedings of the Symposium on VLSI Technology 1990* (IEEE, Piscataway, NJ, 1990), p. 64.
[6] E. C. Jones, S. Ogawa, P. Ameika, M. L. A. Dass, D. B. Fraser, and N. W. Cheung, Mater. Res. Soc. Symp. Proc. **342**, 339 (1994).
[7] J. M. Shannon, Solid-State Electron. **19**, 537 (1976).
[8] E. C. Jones, D. B. Fraser, and N. W. Cheung, J. Electron. Mater. **24**, 863 (1995).
[9] J. M. Stork and R. D. Isaac, IEEE Trans. Electron Devices **30**, 1527 (1983).
[10] L. C. Zhang, C. L. Liang, S. K. Cheung, and N. W. Cheung, J. Vac. Sci. Technol. B **5**, 1716 (1987).
[11] S. Wang, *Fundamentals of Semiconductor Theory and Device Physics* (Prentice-Hall, Englewood Cliffs, NJ, 1989).
[12] S. M. Sze, *Physics of Semiconductor Devices* (Wiley, New York, 1981).